

Histological Effects of Sofosbuvir on The Kidney of Male Albino Rats and The Possible Protective Role of Vitamin C

Gamal Soliman Hassan El Gharabawy, Ezz Elden Alsharkawy Abdallah,
Hassan Fathy Kaabo, Ahmed Mohamed Ahmed Abdel Aleem*

Department of Histology, Faculty of Medicine- Al Azhar University

*Corresponding author: Ahmed Mohamed Ahmed Abdel Aleem; Mobile: (+20)1062656364;

Email: dr_hendawy86@yahoo.com

ABSTRACT

Aim of the work: hepatitis C virus (HCV) infection is a major worldwide public health issue. Direct Acting Antiviral Drugs (DAA) is a revolution that occurred in treatment of hepatitis C virus (HCV). The Second class of DAA is HCV NS5B polymerase inhibitors (Which included Sofosbuvir) was shown to be effective in suppression of HCV replication and became an important component of currently recommended regimens.

Material and Methods: forty adult male albino rats (*Rattus norvegicus*) weighting 140 ± 20 g were selected for this 36-days experiment The rats were randomly categorized into six groups (10 animals each for the first four groups and the remaining groups V&VI were served as the recovery groups). The kidney was excised and prepared in two different techniques for light & electron microscopic examination. For light microscopy serial sections (5 um thick) were stained with hematoxylin-Eosin technique for studying the morphological changes; periodic Acid Schiff technique (PAS) for studying of general carbohydrate ; Masson's trichrome stain for detecting the collagen fibers and transmission electron microscopy (TEM) to detect the ultrastructural changes induced by Sofosbuvir.

Results: the present study showed that group II which received the therapeutic dose of Sofosbuvir (0.06 mg/gm./body weight) showed renal tubular affection compared to the control rats. Tubular affection included massive tubular vacuolization especially cells of the proximal and distal convoluted tubules. Group III which received the toxic dose of Sofosbuvir (0.25 mg/gm./body weight) resulted in glomerular affection compared to the control rats.

Conclusion: the present study provided promising results about reduction of Sofosbuvir nephrotoxicity by the concomitant use of vitamin C.

Keywords: hepatitis C virus (HCV) infection, Sofosbuvir, vitamin C, rat, kidneys, histology .

INTRODUCTION

Egypt has the highest HCV prevalence worldwide which was estimated nationally at 4.1%. HCV genotype 4 is also the predominating strain in Egypt as has been revealed in more than 90% of the infections⁽¹⁾. Treatment of hepatitis C has evolved over the years. An initial study used IFN monotherapy. Subsequently, combination of ribavirin and IFN or of IFN to which polyethylene glycol (PEG) molecules have been added (ie, PEG-IFN) were used⁽²⁾.

Revolution had occurred in the last decade for treatment of hepatitis C virus (HCV) infection by introduction of the direct acting antiviral drugs⁽³⁾. The Second class of direct acting antiviral drugs indicated for HCV infection was HCV NS5B polymerase inhibitors, which included Sofosbuvir which was shown to be effective in suppression of HCV replication and became an important component of currently recommended regimens. Unfortunately, Sofosbuvir had some side effects which included carcinogenesis , mutagenesis, impairment of fertility, pancytopenia, severe depression , disturbances in lactic acid homeostasis with presentations ranged from asymptomatic chronic hyperlactatemia to acute life-threatening lactic acidosis⁽⁴⁾. In order to minimize side effects of Sofosbuvir, we looked for antioxidant. An study had been promoted the nephro-protective effects of vitamin C⁽⁵⁾.

Vitamin-C is an antioxidant supplement that exhibits its powerful scavenging effects against activated oxygen species and various free radicals by neutralizing ROS and decreasing oxidative damage to cell membranes⁽⁶⁾. Due to the limited information concerning the effect Sofosbuvir on the kidney, the present study was designed to assess changes induced by Sofosbuvir on kidneys of male albino rats and the possible protective effects of vitamin C.

MATERIALS AND METHODS

Forty adult male albino rats (*Rattus norvegicus*) weighting (140 ± 20 g) were selected for this 36-days experiment. The rats were randomly categorized into six groups (10 animals each for the first four groups and the remaining groups V&VI were recovery) and they were orally treated as follows:

Group I: animals served as the control group.

Group II: animals were treated with orally the therapeutic dose of Sofosbuvir group (0.06 mg/gm./body weight) dissolved in 0.9% NaCL daily for 21 days

Group III: animals were treated orally with the toxic dose of Sofosbuvir group (0.25mg/gm. /body weight) dissolved in 0.9% NaCL daily for 21 days.

Group IV: animals were treated with orally the therapeutic dose of Sofosbuvir plus vitamin C, in which rats were administrated orally the therapeutic dose of Sofosbuvir (0.06 mg/gm./body weight) plus

vitamin C (0.15 mg/gm./body weight) dissolved in 0.9% NaCL daily for 21 days.

Group V: the first recovery group in which some animals administrated the therapeutic dose group (Group II) and they were treated with 0.9% NaCL daily for another 15 days.

Group VI: the second recovery group in which rats of group IV (The toxic dose group) were treated with 0.9% NaCL daily for another 15 days.

At the determined end date for each group, all rats were sacrificed after ether inhalation. A mid line incision was done. The kidney was excised and prepared in two different techniques for light and electron microscopic examination.

Light microscopy:

Small specimens from the cortex of the right kidney were fixed in 10% neutral buffered formalin overnight, dehydrated, cleared, and embedded in paraffin wax. Serial sections (5 μ m thick) were cut using a rotatory microtome and stained with:

- Hematoxylin-Eosin technique for studying the morphological changes ⁽⁶⁾.
- Periodic Acid Schiff technique (PAS) used for detecting PAS +ve materials ⁽⁶⁾.
- Masson's trichrome stain for studying collagen fibers ⁽⁶⁾.

2- Electron microscopy:

For transmission electron microscopy, small fragments from the cortex of the left kidney were fixed in 2.5% buffered glutaraldehyde dehydrated and embedded in resin.

Semi thin sections (1 μ m) were stained with toluidine blue and used for selection of fields examined by transmission electron microscope (TEM).

Ultrathin sections (6080- nm) were stained with uranyl acetate and lead citrate for examination by JEOL-JEM-100 SX TEM in the electron microscopy unit at the faculty of Medicine, Al-Azhar University, Egypt.

RESULTS

Group I (The control group): light microscopic results

Hx &E stained sections of the kidneys of control rats showed normal structure of the renal corpuscles, proximal and distal convoluted tubules in the cortex (**Figure1**).

PAS stained sections of kidneys of the control rats showed positive PAS materials in the apical and basal membranes of the proximal and distal tubule cells and brush borders of the proximal tubules (**Figure2**).

Masson's trichrome stained sections of kidney cortex of control rats showed normal distribution of collagen fibers in the capsular wall, peritubular and around the blood vessels within the renal cortex (**Figure3**).

Electron microscopic examination of the renal cortex of the control group showed normal renal corpuscle which contained glomerular capillaries that were lined with fenestrated endothelial cells and covered by the cell bodies of podocytes. (**Figure4**). The proximal (PCTs) and distal convoluted tubules (DCTs) were lined with cubical cells that had rounded euchromatic nuclei, numerous longitudinally oriented mitochondria were found at the basal part of the cells between the basal cell membrane enfolding. Numerous long microvilli were seen projecting from the luminal surface of PCTs (**Figures 5,6**).

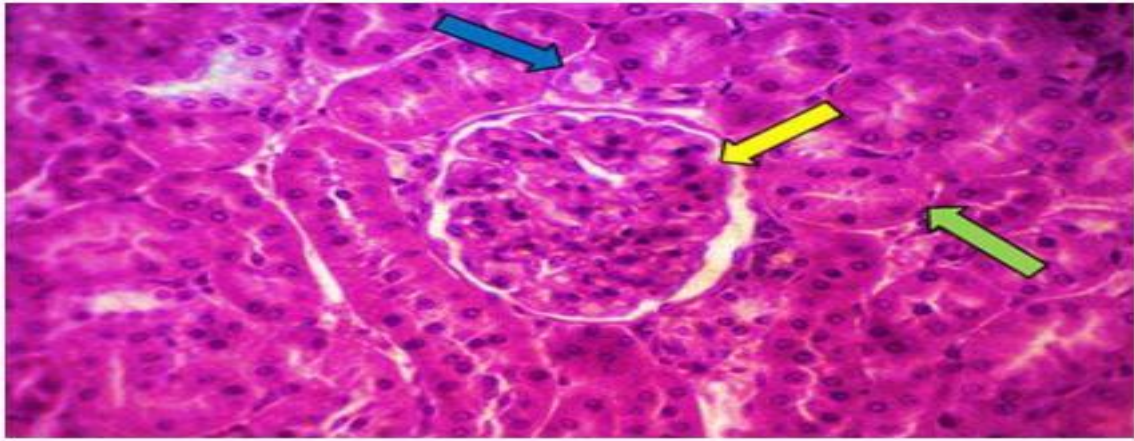


Figure 1: A photomicrograph of kidney cortex of male albino rat of the control group showing the glomerular tuft of capillaries (Yellow arrow) surrounded by Bowman's capsule. Renal tubules are proximal (Green arrow) and distal (Blue arrow) (H&E stain X400)

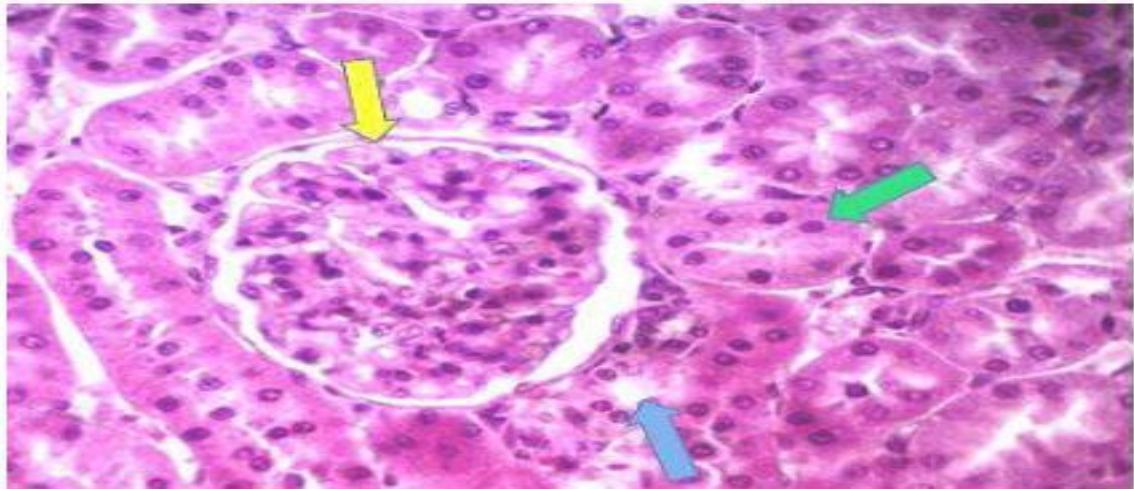


Figure 2: a photomicrograph of section in kidney cortex of male albino rat of the control group showing PAS positive materials in glomerulus (Yellow arrow), proximal tubules (Green arrow), distal tubules (Blue arrow) and brush border of proximal tubule (PAS stain X 400)

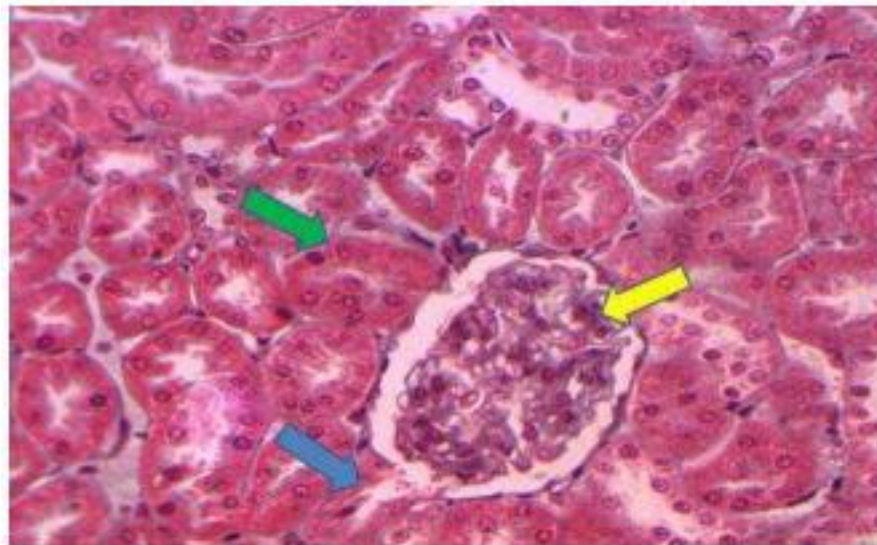


Fig. 3: a photomicrograph of a section in kidney of male albino rat from control group showing thin collagen fibers supporting the glomerulus, in Bowman's capsule and basement membrane of the cuboidal cells around renal tubules (Masson's trichrome stain X400)

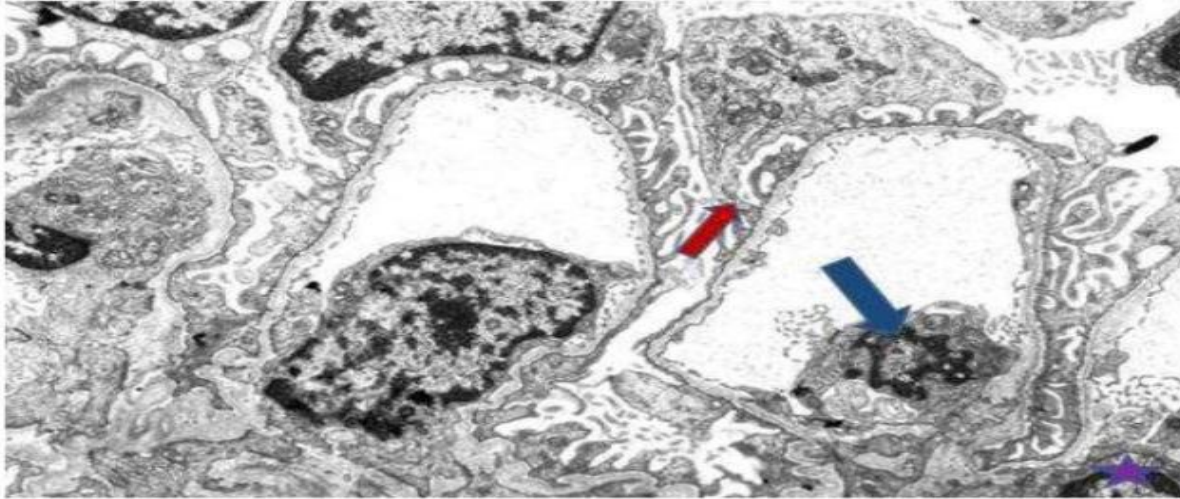


Fig.4: electron micrograph of section in kidney cortex of male albino rat from the control group showing intact Podocyte's foot processes (red Arrow), capillary loops which lined by endothelial cells (blue Arrow). Mesangial cells (star) support the capillary loops (X 8120).

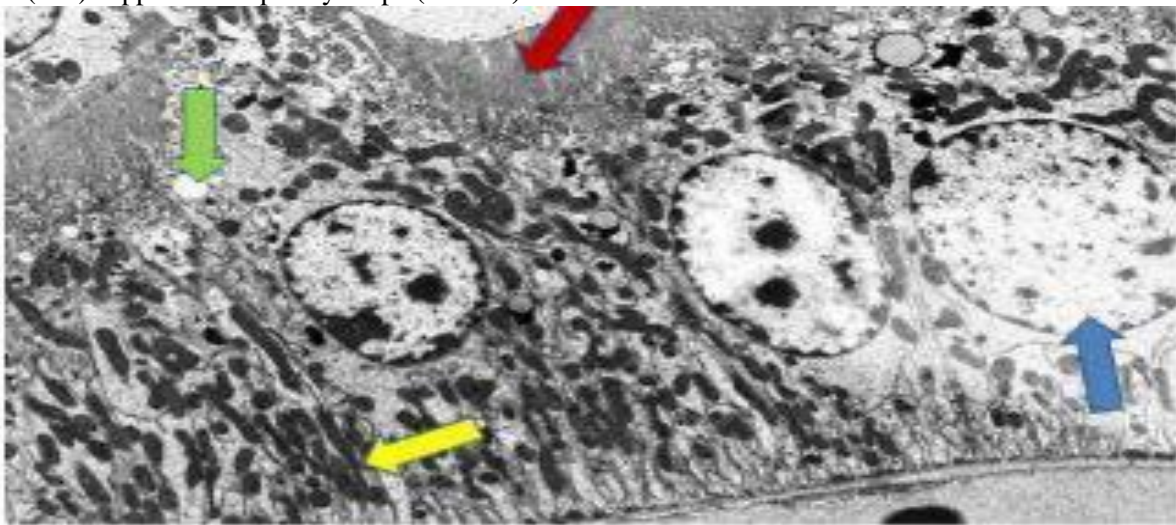


Fig.5: electron micrograph of section in kidney cortex of male albino rat from the control group showing PCTs lined with cubical cells that had rounded nuclei (Blue arrow), longitudinal mitochondria (Yellow arrow) at the basal part of cells between the basal cell membrane enfolding. lysosomes (Green arrow) also are found in the cytoplasm with long microvilli (Red arrow) projecting from the luminal surface of PCTs (X 2000).

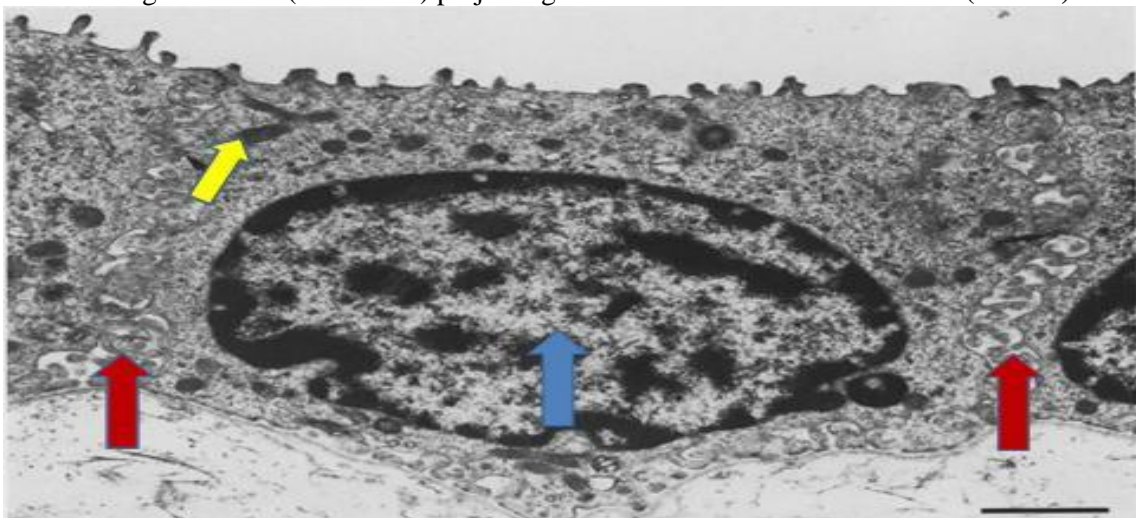


Fig.6: electron micrograph of Section in kidney cortex of male albino rat from the **control** group showing the DCT: cell is cuboidal with rounded nuclei (Blue arrow),the cytoplasm contains only a few mitochondria (Yellow arrow), lateral micro folds protruding into the lateral intercellular space (Red arrows) and enfolding also to the basal cell membrane (X 4000).

Group 2: Light microscopic results

- **Hx &E** stained sections of kidneys of rats of group II: rats showed a little affection of glomeruli with widening of the Bowman's spaces. The PCTs showed loss of microvilli of PCTs with tubular vacuolization especially in cells of the proximal and distal convoluted tubules, lumens of some PCTs contained remnants of degenerated epithelial cells. Their nuclei showed dark staining affinity with different degrees of degeneration and karyolysis (**Figure7**).
- **PAS** stained sections of kidneys of rats of group II showed a weak PAS reaction in the apical membranes with increased staining affinity in the basal membranes of the proximal and distal convoluted tubular cells. A moderate reaction in the distorted glomeruli was also observed (**Figure8**).
- **Masson trichrome** stained sections of the kidney of rats of group II showed mild increase in collagen

fibers around the renal corpuscles and the renal tubules as well as increased collagen fibers between the glomerular capillaries as compared to the control group (**Figure9**).

- **Electron microscopic examination** of the renal cortex of group II showed a thickening in the glomerular capillary basement membranes, and fusion of the capillary endothelial cells and fusion of some Podocyte's pedicles (**Figure10**). The PCTs showed areas of complete loss of microvilli, cytoplasmic empty areas, vacuoles, swollen mitochondria and loss of normal mitochondrial arrangement between the basal membrane enfolding's. Some nuclei appeared shrunken, heterochromatic and others appeared with few chromatins (**Figures11,12**).

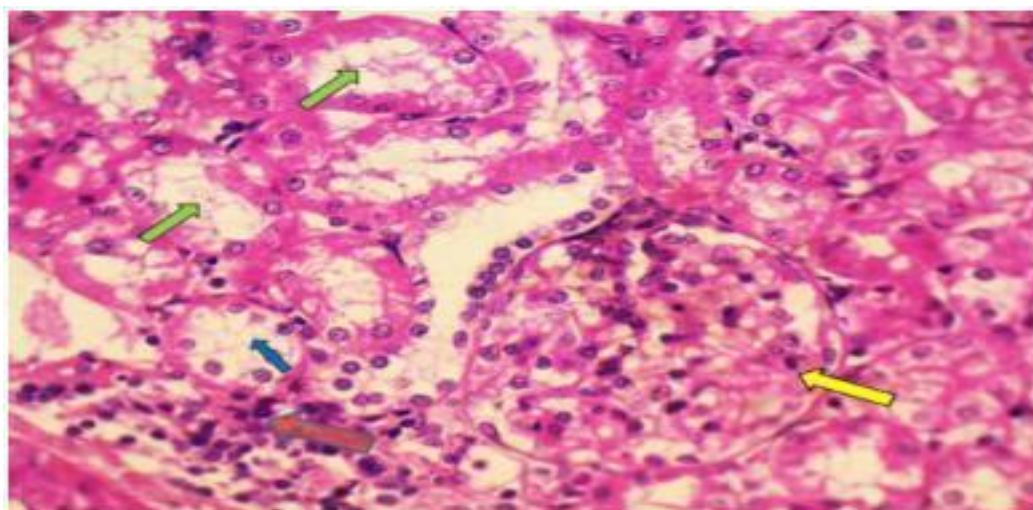


Figure7: a photomicrograph of kidney cortex of male albino rat of group II (ThDS) showing massive tubular vacuolization especially cells of the proximal (Green arrow) and distal (Blue arrow) convoluted tubules accompanied with lymphocytic infiltration (Brown arrow) with hypertrophied glomerulus and undetected Bowman's capsule (Yellow arrow) (**H&E X400**).

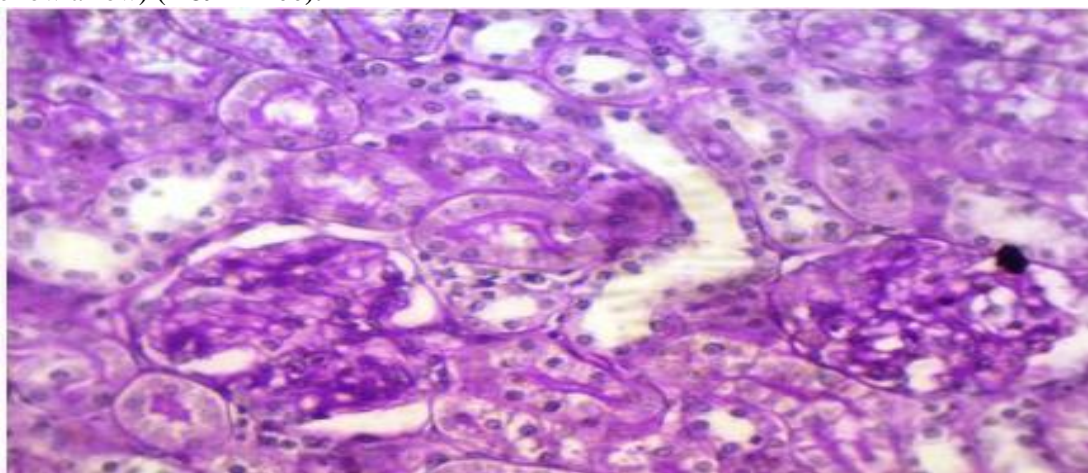


Figure 8: a photomicrograph of kidney cortex of male albino rat of group II (ThDS) with decreased of PAS +ve materials in the apical membrane but looks stronger in the basal membranes of the proximal and distal convoluted tubular cells. A moderate reaction in the distorted glomerulus is also observed (**PAS reaction X400**).

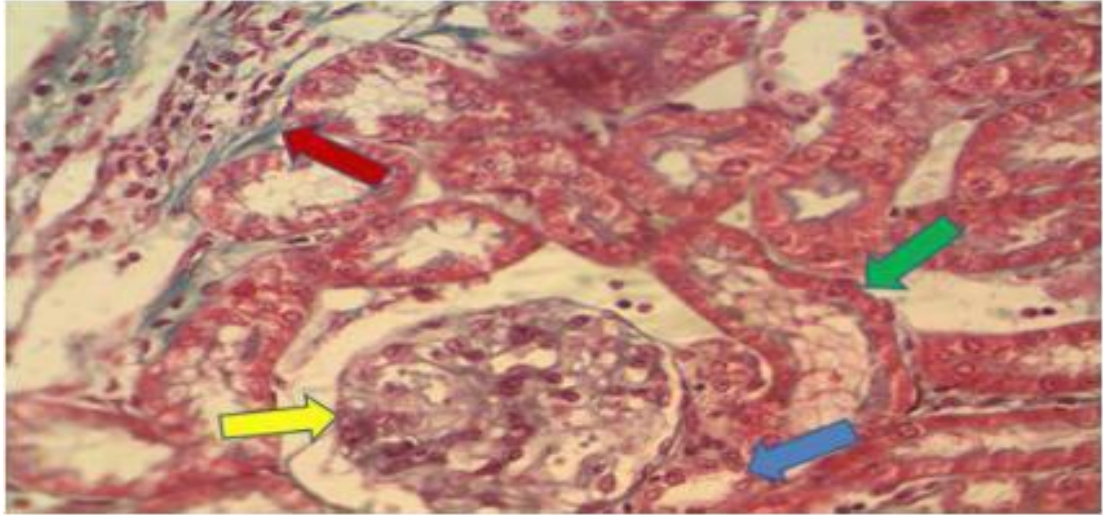


Fig. 9: a photomicrograph of kidney cortex of male albino rat of group II showing increased collagen fibers in interstitium (Red arrow), in the glomerulus (Yellow arrow) and in the basement membranes of the convoluted tubules (Masson's trichrome stain X400).

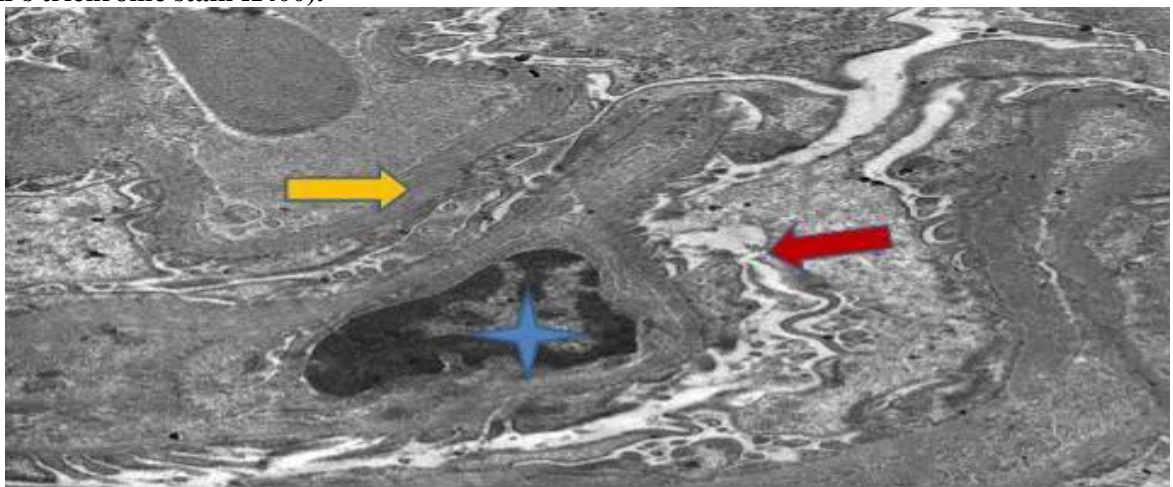


Fig.10: electron micrograph of kidney cortex of male albino rat from the group II showing destroyed Podocyte's primary and secondary processes (Red arrow) with thickened capillary basement membrane (Yellow arrow) and corrugated nuclear membrane of the endothelial lining (Star) (X7000).

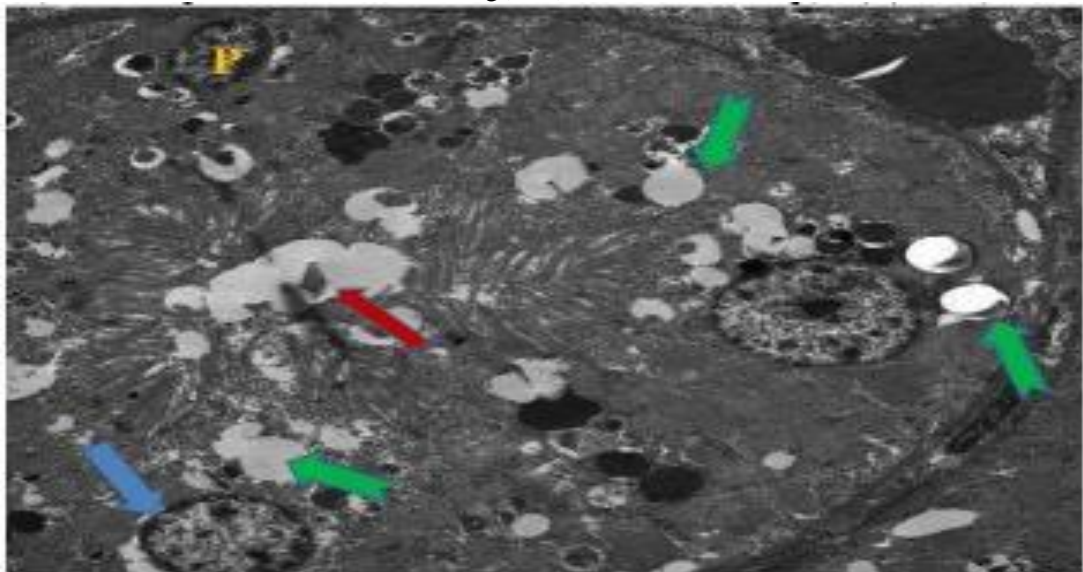


Fig.11: electron micrograph of kidney cortex of male albino rat of group II showing lining cells of proximal convoluted tubules with distorted brush borders (Red arrow) with increased lysosomal cytoplasmic vacuolization (Green arrow) and some pyknotic (P) and karyolytic nuclei (Blue arrow) (X 3000).

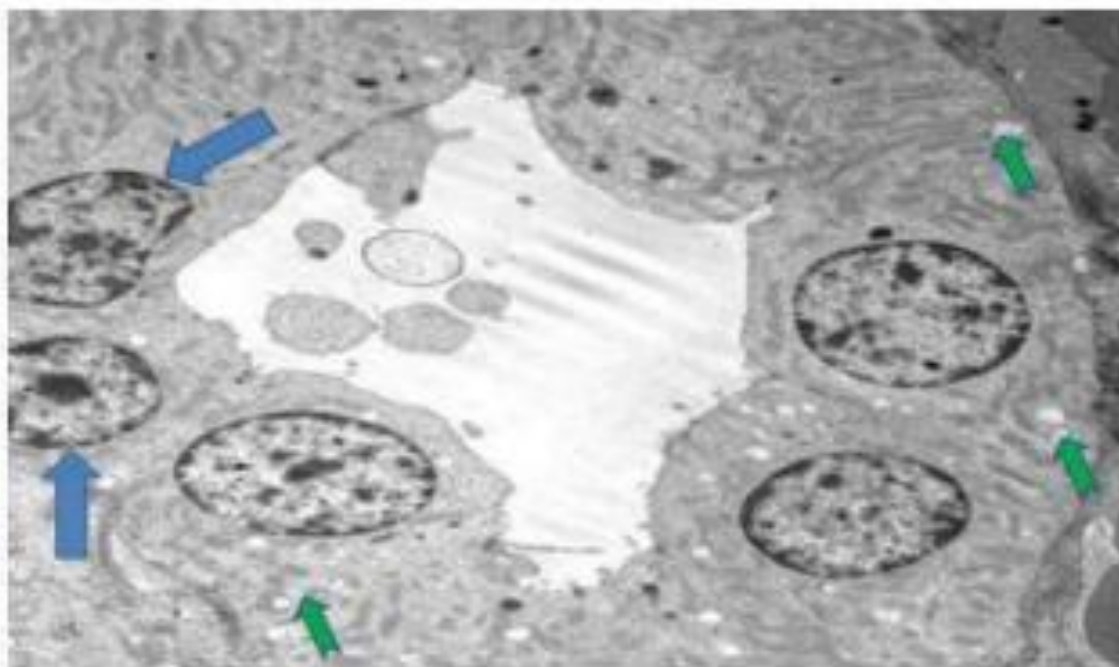


Figure 12: electron micrograph of kidney cortex of male albino rat of group II showing lining cells of distal convoluted tubules with cytoplasmic vacuolization (Green Arrow) and some pyknotic nucleus (Blue arrow), karyolysis while few or no microvilli are seen in DCTs with debris of degenerated epithelial cells are detected in the lumen(X 5000)

Group 3: toxic dose of Sofosbuvir group

Light microscopic results

- **Hx & E** stained sections of kidney cortex of group III: rats showed marked structural changes in the renal corpuscles and some convoluted tubules. There was marked atrophy, destruction and irregular outline of the glomeruli with widening of some areas of the capsular space. Severe damage was observed in many corpuscles in the form of irregularity and shrinkage with loss of their vascular components. Some of epithelial cells of the proximal and distal tubules showed features of vacuolization (**Figure13**).
- **PAS** stained sections of the kidneys of group III: rats showed A marked decrease of PAS +ve materials with negatively stained glomeruli (**Figure14**).

- **Masson's trichrome** stained sections of kidneys cortex of group III: rats showed marked increase of the collagen fibers in interstium around the capsular wall, peritubular and around the blood vessels in the cortex (**Figure15**).

Electron microscopic examination of the renal cortex of group III showed prominent glomerular changes. The glomeruli showed thickened Glomerular basement membrane (Gbm). Also, capillary lumens were obliterated by end capillary hyper cellularity and hypertrophy with fusion of secondary foot processes and mesangial hyper cellularity (**Figure16**). The renal tubules revealed minimal changes. The lining cells of proximal convoluted tubules showed partial loss of microvilli, minimal cytoplasmic vacuolization and few degenerated mitochondria and abnormal pyknotic nuclei (**Figures17,18**).

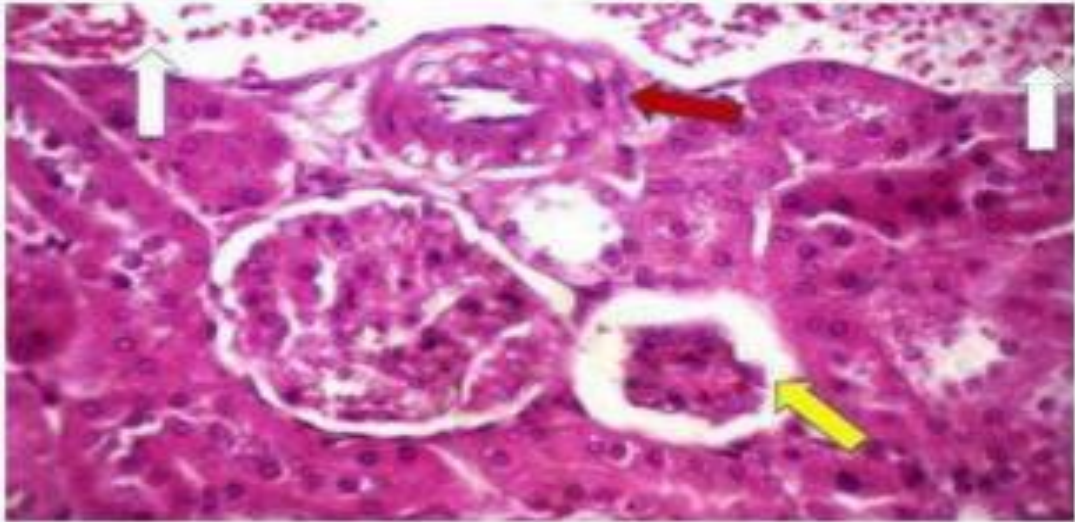


Figure 13: a photomicrograph of kidney cortex of male albino rat of group **III** (TDS), showing atrophy and destruction of glomeruli, widening of the capsular space (yellow arrow) with interstitial hemorrhage (White arrow). Also, there is thickening and edema of the arterial wall (Red arrow) with numerous pyknotic nuclei of cells of the convoluted tubules (**Hx&E stain X400**)

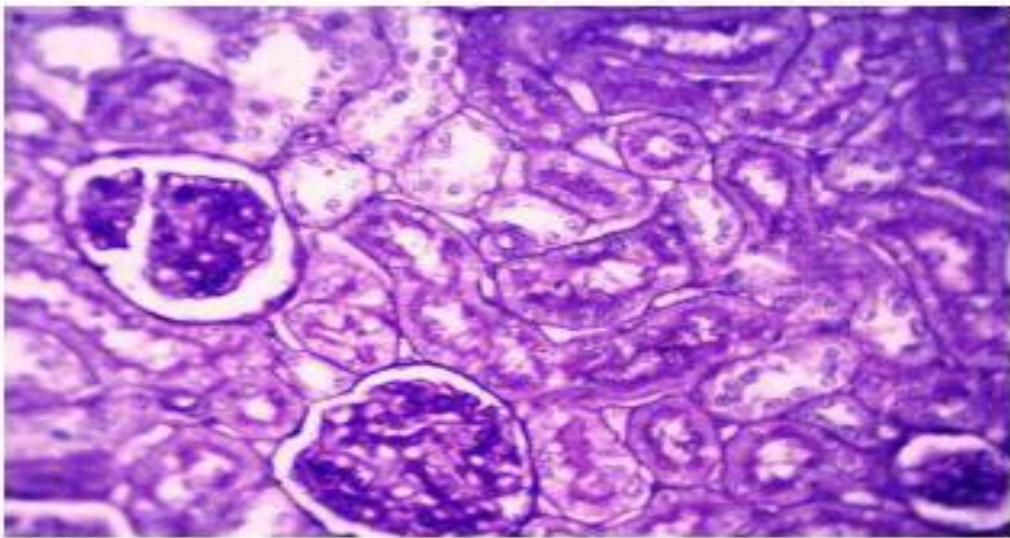


Figure 14: a photo micrograph of kidney cortex of male albino rat of group **III** showing decreased PAS +ve materials with negatively stained glomeruli (**PAS stain X400**)

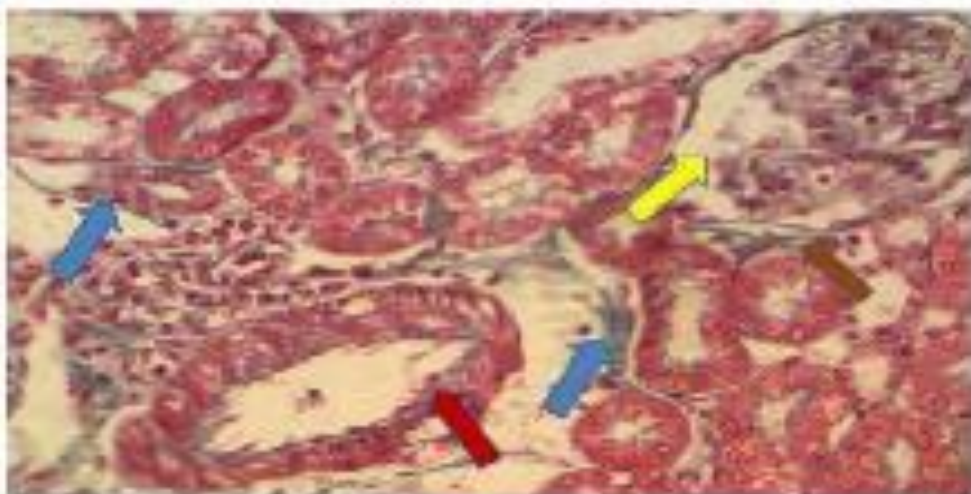


Fig. 15: a photomicrograph of kidney cortex of male albino rat from group **III** showing marked increase of the collagen fibers around glomerulus (orange arrow) and renal tubules (Blue arrow) and the arterial wall (Red arrow) Also, there is partial destruction of glomerulus (Yellow arrow) (**Masson's trichrome stain X400**).

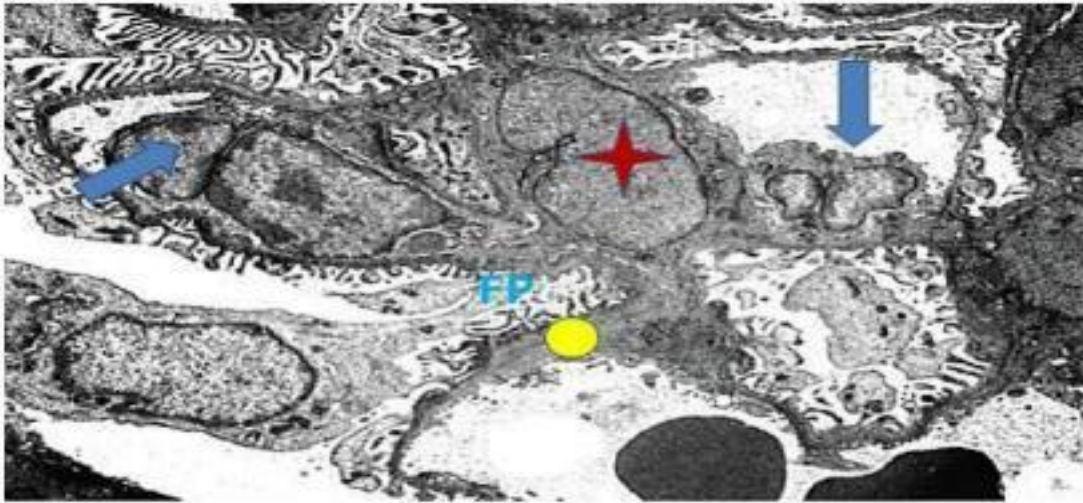


Fig.16: electron micrograph of kidney cortex of male albino rat from the group **III** showing thickened renal glomerular basement membrane (Circle), capillary endothelial lining contained hypertrophied nuclei (Blue arrow) also fusion of secondary foot processes (FP) and mesangial hypercellularity (Star) (X 5000).

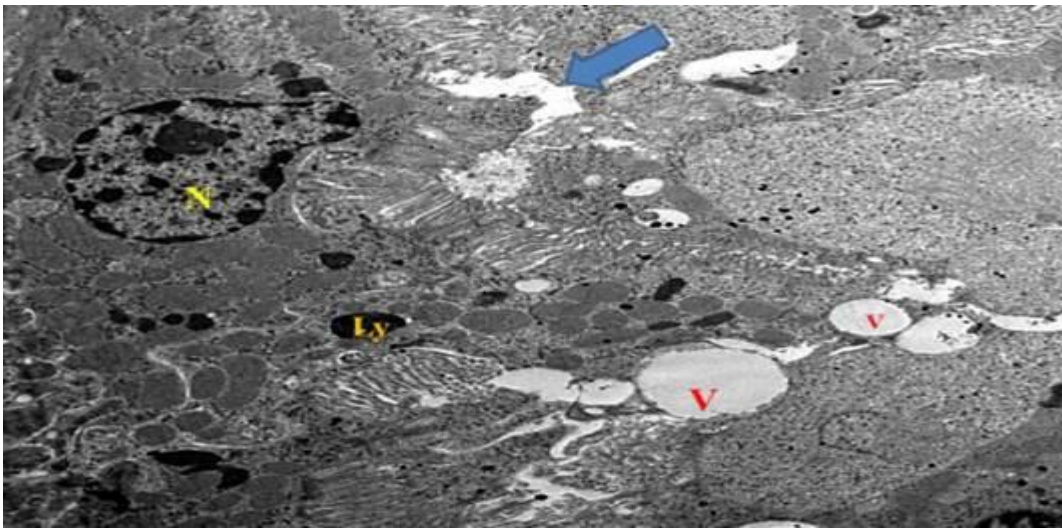


Fig.17: electron micrograph of kidney cortex of male albino rat from the group **III** showing cells of the proximal convoluted tubule which contains large cytoplasmic vacuoles (V), numerous lysosomal bodies (Ly), nucleus (N) with fragmented chromatin and partial destruction of the brush border (Blue arrow) (X 4000).

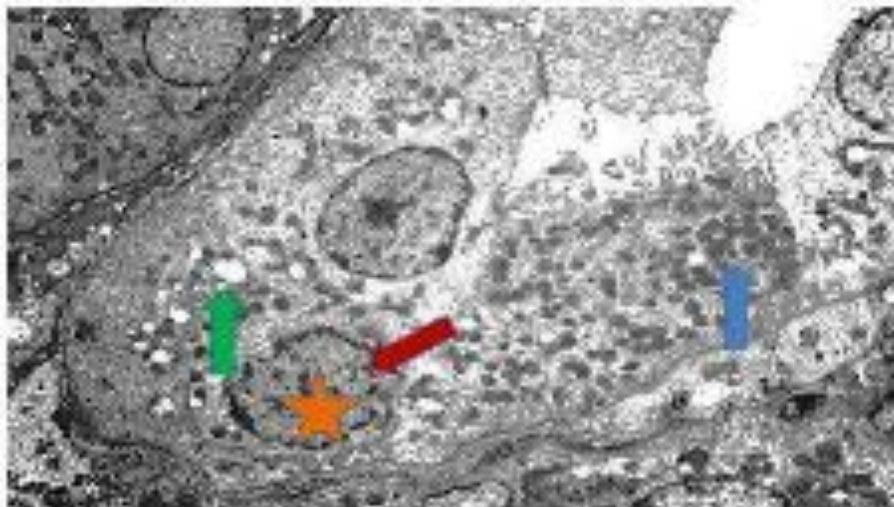


Fig.18: electron micrograph kidney cortex of male albino rat from group **III** showing epithelial lining of the distal tubule with cytoplasmic vacuolization (Green arrow), deformed mitochondria (Blue arrow) and some karyolytic nucleus (Star) with corrugated nuclear membrane (Red arrow) (X 3000).

Group IV: therapeutic dose of Sofosbuvir group plus vitamin C.

Light microscopic results:

- **Hx. &E** stained sections of kidney cortex of group IV: some of the proximal and distal convoluted tubules presented with mild vacuolization. Moreover, the brush borders of proximal tubule epithelial cells were still intact and the glomerular capillary tufts nearly looks similar to that of the control group (**Figure19**).
- **PAS** stained sections of the kidneys of group IV: rats showed decreased PAS reaction in the apical and basal membranes of the proximal and distal tubule cells as well as in the glomerular tufts comparable to the control (**Figure 20**).

Masson's trichrome stained sections of the kidney cortex of group IV: rats showed fine and scattered collagen fibers around the renal corpuscle and the renal tubules can be hardly seen as comparable with the control group (**Figure 21**).

Electron microscopic examination of the renal cortex of group IV showed well maintained ultrastructure of kidney. The glomerular basement membranes, the lining endothelium of capillaries and the Podocyte's pedicle appeared intact to some extent (**Figure 22**). PCTs displayed intact microvilli, mitochondria and nuclei (**Figure 23**). The DCTs had a conserved ultrastructure. The cytoplasm contains elongated mitochondria & small lysosomes also, lateral and basal cell membrane enfolding and minimally corrugated nuclear envelope (**Figure 24**).

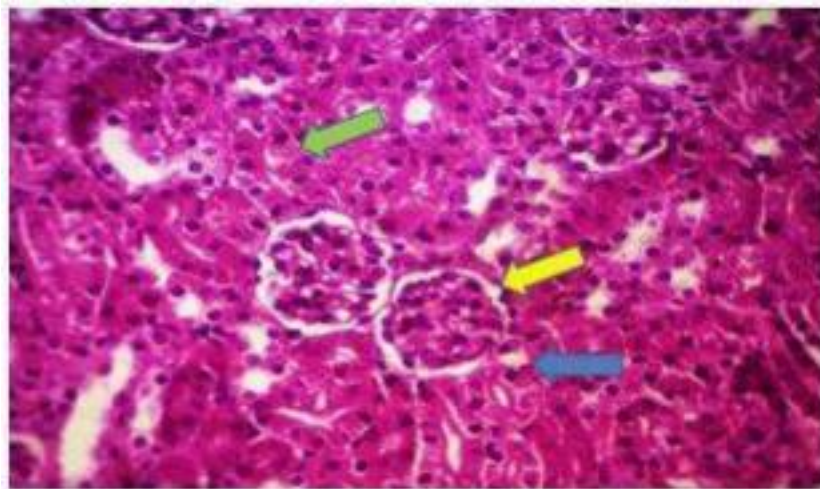


Figure 19: photo micrograph kidney cortex of male albino rat of group IV showing normal Bowman's capsule including glomerulus (Yellow arrow), but some of proximal (Green arrow) and distal (Blue arrow) convoluted tubules show mild vacuolization (**Hx &E stain X 400**).

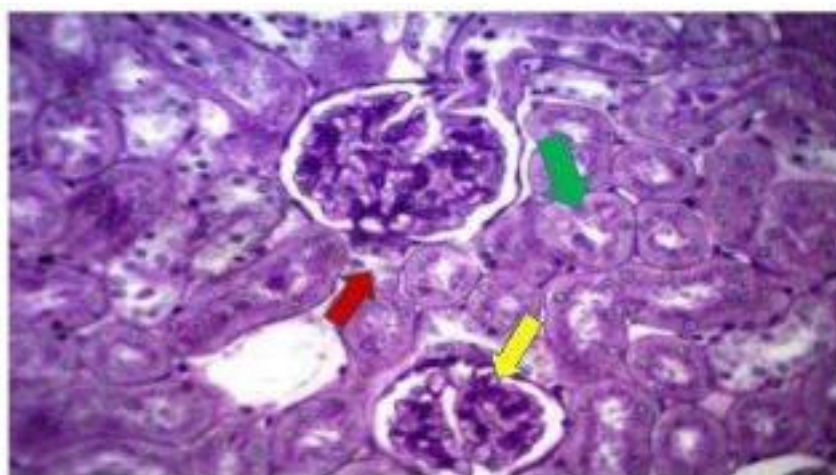


Figure 20: photo micrograph of kidney cortex of male albino rat of group IV showing mild decrease of PAS +ve materials in the apical and basal membranes of the proximal (Green arrow) and distal tubule cells (Red arrow) as well as in the glomerular tufts (Yellow arrow) comparable to the control (**PAS stain X400**).

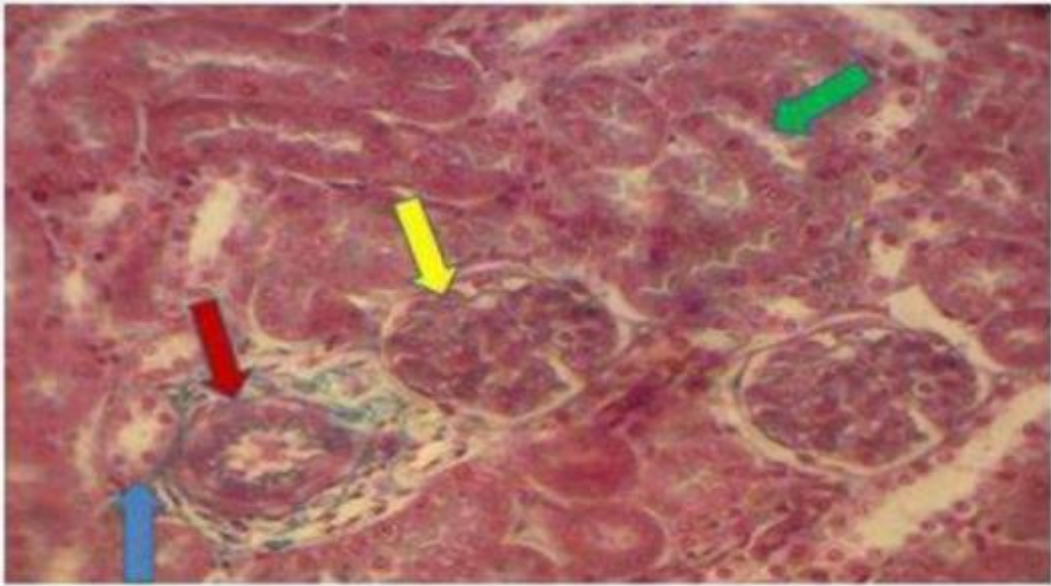


Fig. 21: a photomicrograph of kidney cortex of male albino rat from group IV showing minimal amount of collagen around afferent arteriole (Red arrow), normal capillary tuft of glomerulus (Yellow arrow) with normal proximal (Green arrow) and distal tubules (Blue arrow) (Masson's trichrome stain X400)

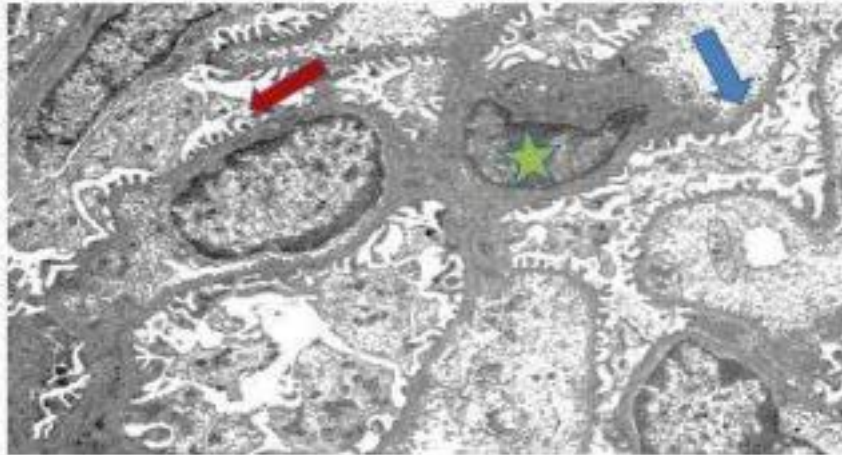


Fig.22: electron micrograph of kidney cortex of male albino rat from the group IV showing Podocyte's with nearly regular foot processes (Red arrow) some pyknotic nucleus of capillary endothelium (Star) and slight thickening of GBM (Blue arrow) (X 5000)

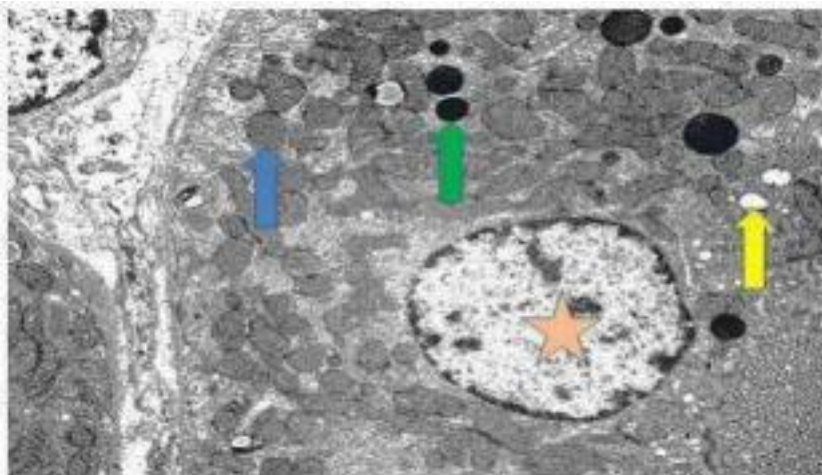


Fig.23: electron micrograph in kidney cortex of male albino rat from the group IV showing cells of proximal convoluted tubule with lysosomes (Green arrow). Nucleus (Star), numerous mitochondria (Blue arrow) and small vacuoles beneath the intact brush border microvilli (Yellow arrow) (X 3000)

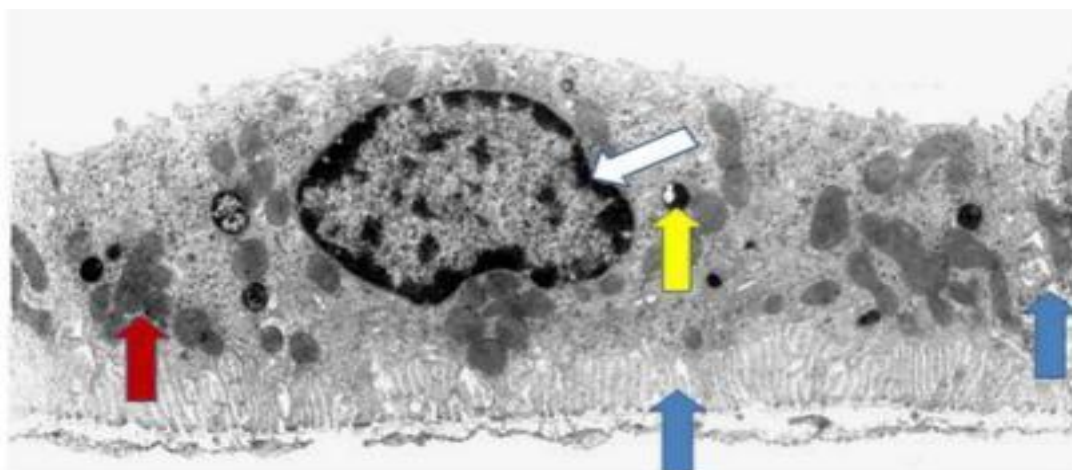


Fig.24: electron micrograph of kidney cortex of male albino rat from the group IV showing epithelial lining of distal tubule. The cytoplasm contains elongated mitochondria (Red arrow) & small lysosomes (Yellow arrow) also, lateral and basal cell membrane enfolding (Blue arrow) and minimally corrugated nuclear envelope (White arrow) (X 4000).

Group V: first recovery group

Light microscopic results:

- **Hx. &E** stained sections of kidneys cortex of group V: rats showed minimal vacuolization in some cells of proximal and distal tubules. The rest of tubules succeeded to return to its normal shape with preserved brush border of proximal tubule. Also, the previously affected glomerular tuft of capillaries shows improvement in their structure (**Figure 25**).
- **PAS** stained sections of the kidney cortex of group V: rats showed starting rise of PAS positive materials in the basement membrane of Bowman's capsule and glomerulus. The renal tubules also showed some signs of recovery especially in the brush border of proximal tubular epithelial cells which appears positively stained (**Figure 26**).
- **Masson trichrome** stained sections of the kidney cortex of group V: rats showed few collagen fibers

around the glomeruli and tubules and looks like control group (**Figure 27**).

- **Electron microscopic examination** of the renal cortex of group V showed improvement in the previous renal tubular insult. There is minimal thickening in the glomerular capillary basement membrane and Podocyte's showed fusion of their foot processes in some areas and in other areas it looks normal (**Figure 28**). Proximal convoluted tubules cells contained large cytoplasmic vacuoles, clusters of deformed mitochondria, numerous lysosomes and lamellar (Myeloid) body, Nucleus revealed condensed chromatin pattern and the brush border of PCTs showed normal architecture (**Figure 29**). The lining cells of distal convoluted tubules which are flattened, and the nucleus show increase in width, the lateral intercellular spaces appear decreased in width as compared to spaces in normal tubules and mitochondria look normal (**Figure 30**).



Figure 25: a photomicrograph of kidney cortex of male albino rat of group V (R1) showing glomerular improvement, but still wide capsular space (Yellow arrow) are realized. The renal tubules show minimal vacuolization in some cells of the distal tubules (Blue arrow) and proximal tubules (Green arrow) and the rest of them succeed to return back to their normal shape, with preserved brush border of the proximal tubule (**H &E stain X400**).

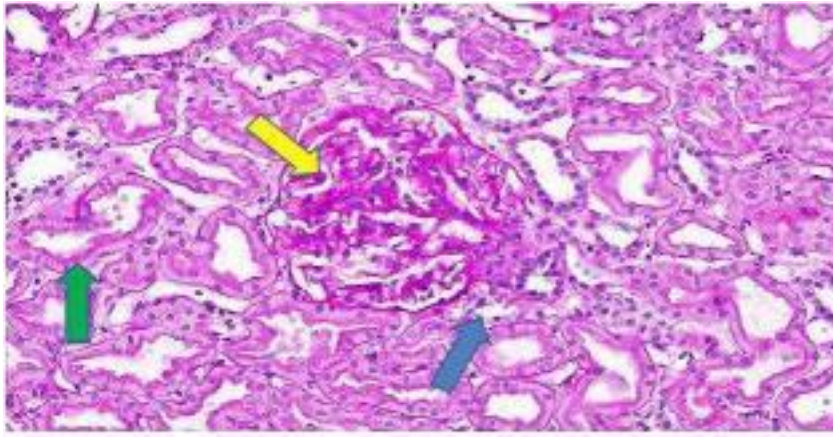


Figure 26: photo micrograph of kidney cortex of male albino rat of group 5 (R1) showing increased PAS positive materials in the basement membrane of Bowman's capsule and glomerulus (Yellow arrow). The renal tubules show some signs of recovery especially in the brush border of proximal tubular epithelial cells (Green arrow) along with distal tubules (blue arrow) (PAS stain X400)

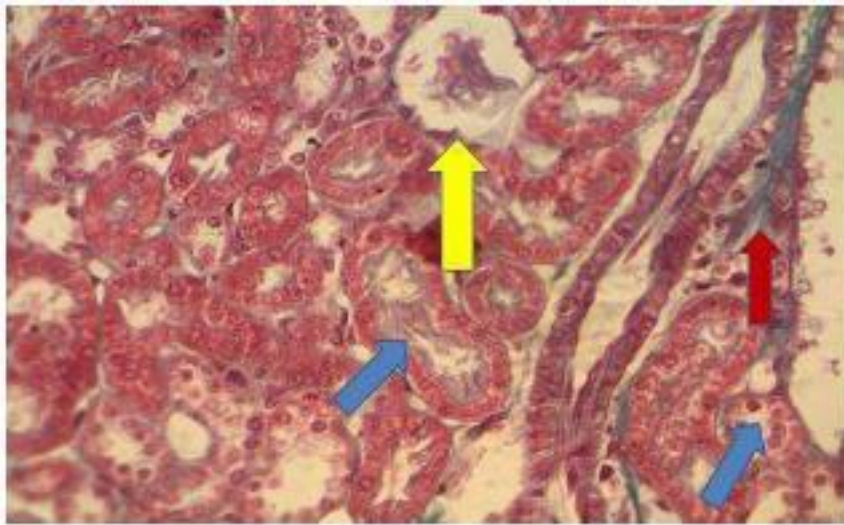


Fig. 27: a photomicrograph of kidney cortex of male albino rat from group V (R1) showing minimal amount of collagen fibers around Bowman's capsule, renal tubules and interstitium (Red arrow) with signs of improvement of tubular vacuolization especially cells of the proximal (Green arrow) and distal (Blue arrow) convoluted tubule, accompanied by stands glomerular affection (Yellow arrow) (Masson's trichrome stain X400)

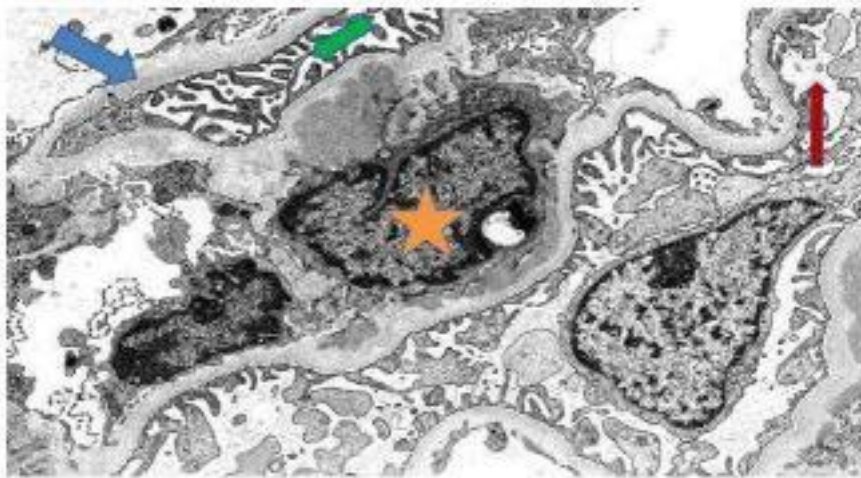


Fig.28: electron micrograph of Section in kidney of male albino rat from the group V (R1) showing thick glomerular capillary basement membrane (Blue arrow). Podocyte's fusion and destruction of their foot processes in some areas (Red arrow) and in other areas it looks normal (Green arrow) also Mesangial cells show abnormal pyknotic nucleus (Star) (X 5000).

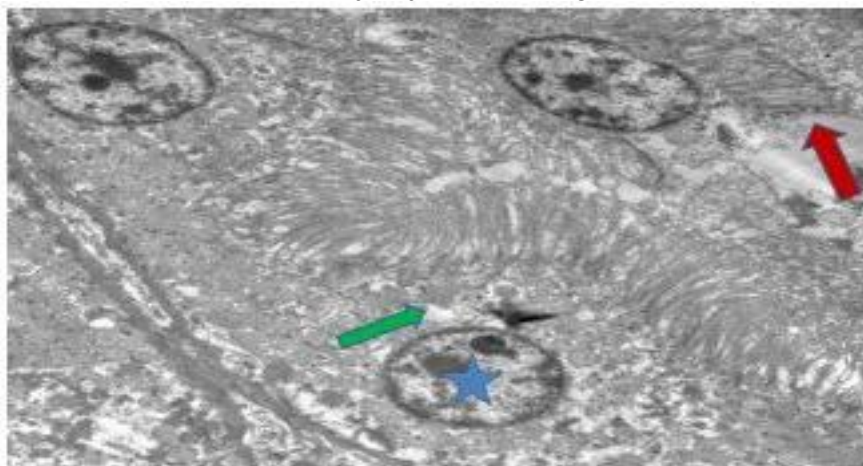


Fig.29: electron micrograph of section of kidney cortex of male albino rat from the group V (R1) showing lining cells of the proximal convoluted tubules with brush border which show normal architecture (Red arrow), few cytoplasmic vacuolization (Green arrow) and their nuclei look like normal ones (Star) (X4800).

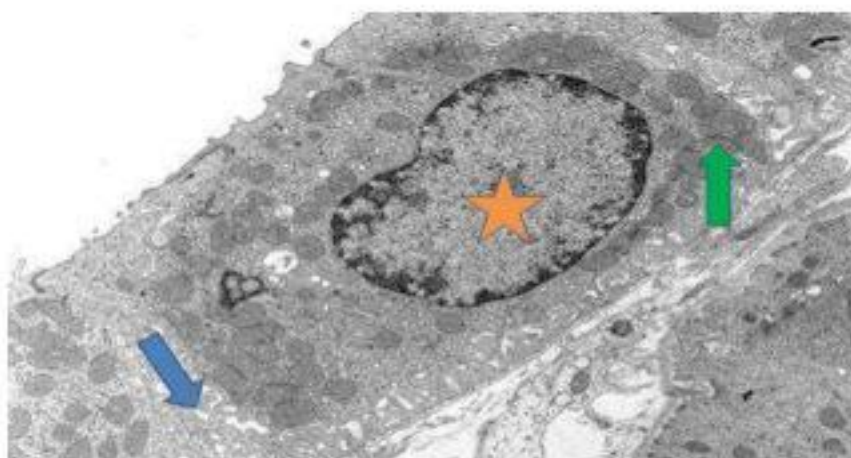


Fig. 30: electron micrograph of section in kidney of male albino rat from the group V (R1) showing lining cells of distal convoluted tubules which are flattened, and the nucleus show increase in width (Star). The lateral intercellular spaces (Blue arrow) appear decreased in width as compared to spaces in normal tubules and mitochondria (Green arrow) look normal (X4800).

Group VI: light microscopic results of the second recovery group:

- **Hx. &E.** stained sections of the kidneys of group VI showed healing of distorted Glomerular tuft of capillaries. Also, there was minimal vacuolization in some cells of proximal and the distal tubules accompanied with well-preserved brush border of proximal tubule in the rest of the tubules (**Figure 31**).
- **PAS** stained sections of the kidneys of group VI: rats showed that the glomerular destruction which occurred early did not recover easily in short time. This presented by some of the glomeruli appeared as recovering with mild PAS reaction and the other glomeruli takes longer time to recover and presented by weak PAS reaction. Also, there was mild PAS reaction in renal tubules with partial affection of brush border of PCT (**Figure 32**).

Masson's trichrome stained sections of the kidneys of group VI: rats showed minimal disappearance of the collagen fibers seen in interstium around the capsular wall, peri tubular and around the blood vessels within the renal cortex (**Figure 33**).

Electron microscopic examination of the renal cortex of group VI showed improvement in previous glomerular affection. The glomerulus appears with minimal thickened GBM, capillaries showed reopening of their lumens. Also fusion of secondary foot processes and mesangial hyper cellularity is diminished (**Figure 34**). The renal tubules revealed minimal changes. The lining cells of proximal convoluted tubules showed regained loss of microvilli, minimal cytoplasmic vacuolization and few mitochondrial affection and normal nuclei (**Figure 35**).

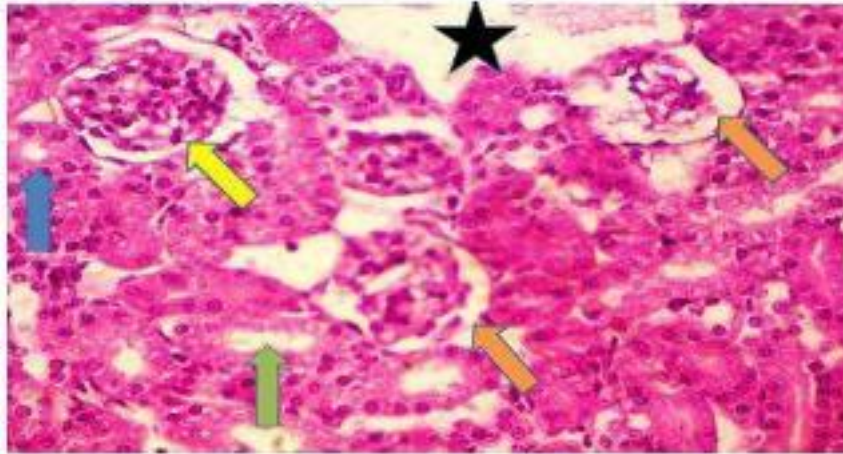


Figure 31: light photomicrography of section in kidney cortex of male albino rat of group VI (R2) showing healing of some previously distorted glomeruli (Yellow arrow) and the rest of glomeruli still affected (Orange arrow). Also, there is empty Bowman's capsule (Star). The renal tubules showing minimal vacuolization in the cells of proximal (Green arrow) and distal tubules (Blue arrow) (**Hx &E stain X400**).

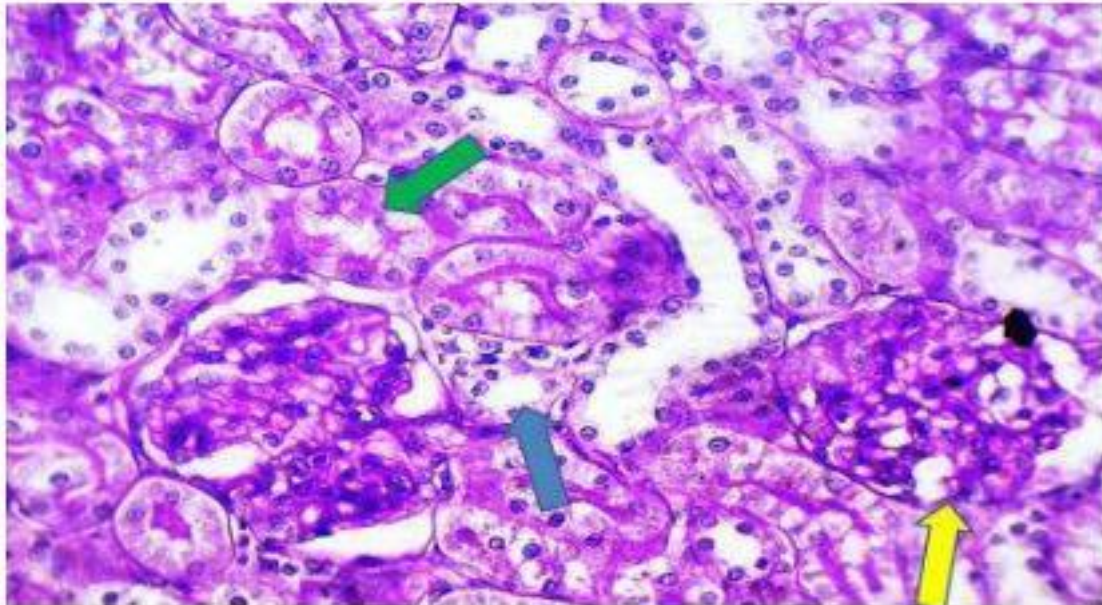


Figure 32: photo micrograph of section in kidney of male albino rat of group VI (R2) showing the recovered glomeruli (yellow arrow) with moderate PAS +ve materials but the renal tubules shows focal affection of DCT (Blue arrow) and PCT especially at their brush border (Green arrow). (**PAS reaction X400**).

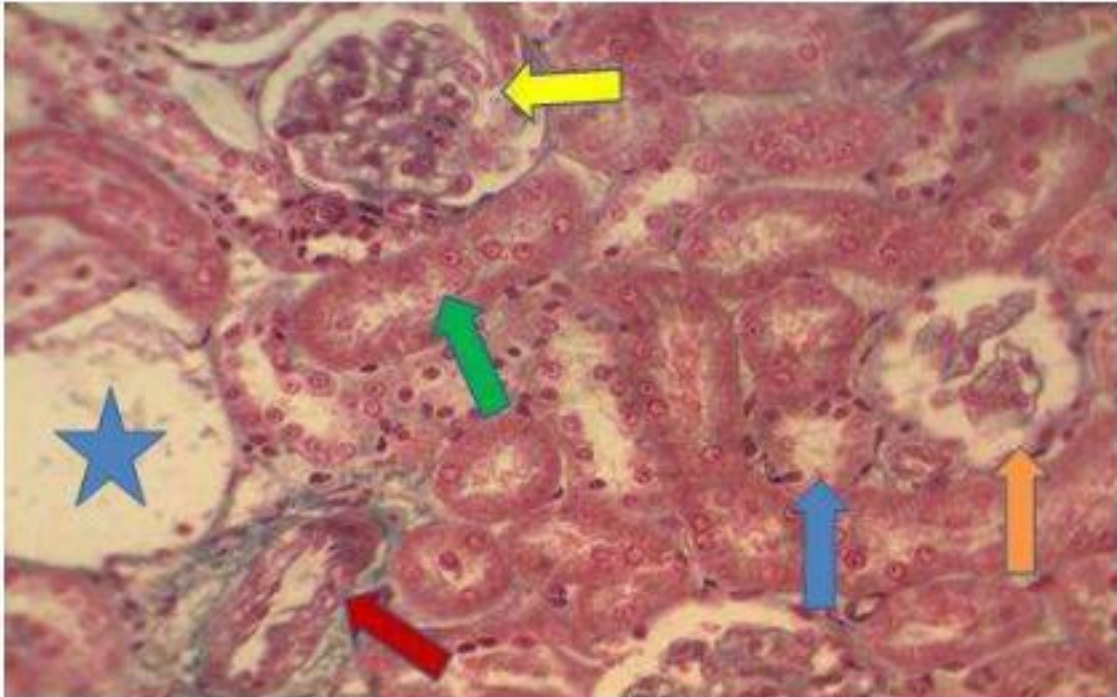


Fig.33: photomicrograph of a section in kidney of male albino rat from group 6 (R2) showing collagen fibers around Blood vessels (Red arrow), Bowman's capsule (yellow arrow). Renal tubules seem normal (green arrow for PCT. & blue arrow for DCT (Masson's trichrome stain X400)

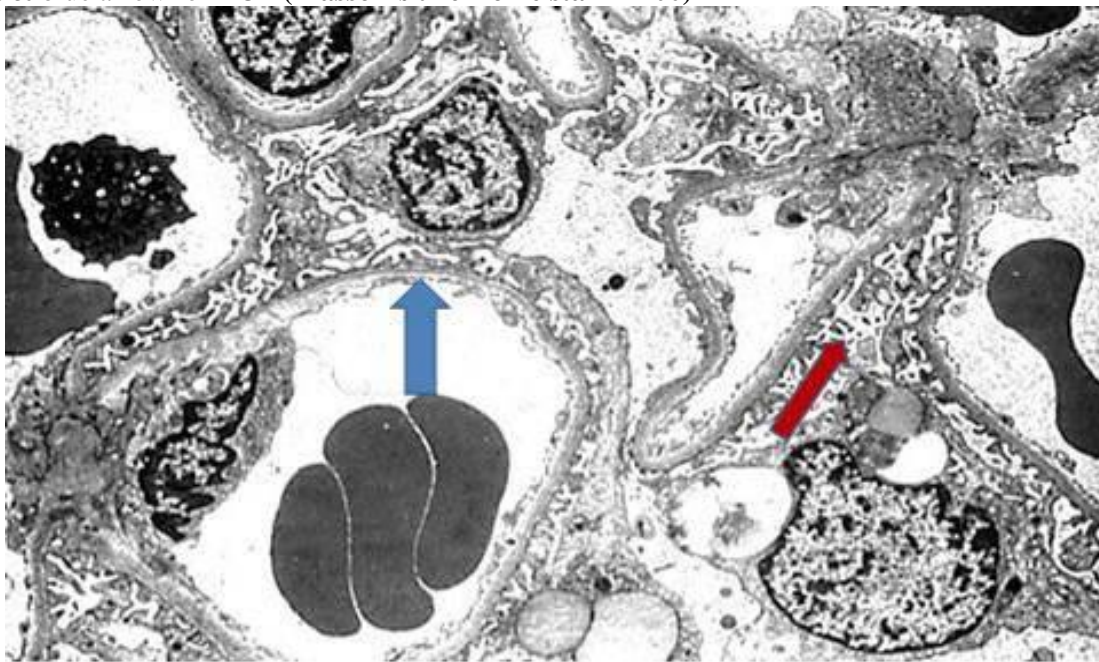


Fig. 34: electron micrograph of section in kidney of male albino rat from the group VI (R2) showing improvement of thickened the glomerular capillary basement membrane (Blue arrow) and Podocyte's foot processes fusion and destruction is not improved (Red arrow) (X 5000).

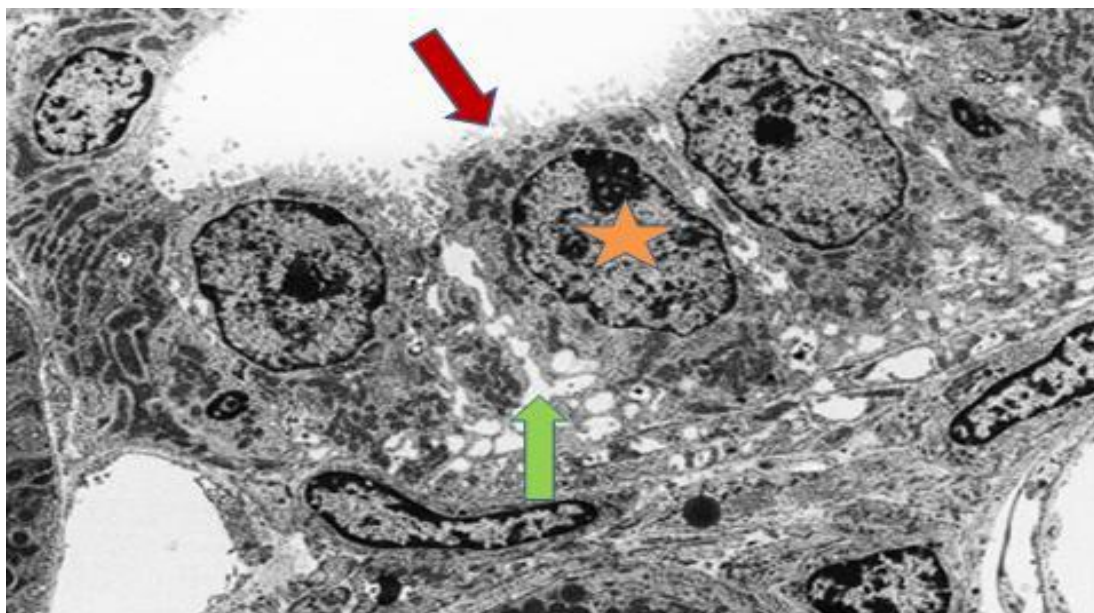


Fig. 35: electron micrograph of Section in kidney of male albino rat from the group VI (R2) showing lining cells of proximal convoluted tubules with lateral and basal cytoplasmic vacuolization (Green arrow) and with brush border still abnormal (Red arrow). Nuclei look like normal ones (Star) (X 2000).

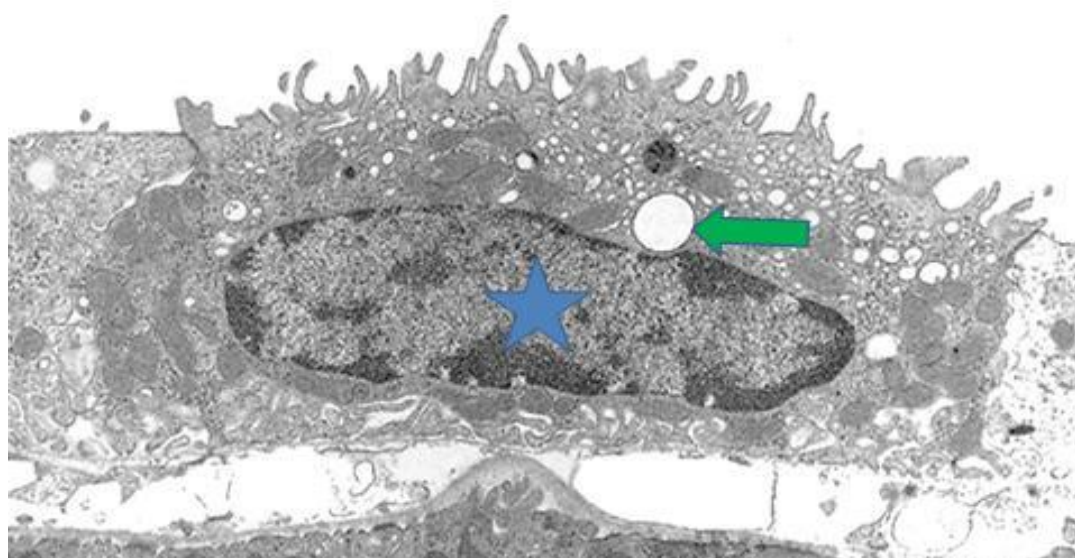


Fig. 36: electron micrograph of Section in kidney of male albino rat from the group VI (R2) showing lining cells of distal convoluted tubules with apical cytoplasmic vacuolization (Green arrow) and abnormal nucleus (Star) (X 4000).

CONCLUSION

Sofosbuvir - treated rats revealed 2 types of affection: tubular (In group II) and glomerular (In group III) affections. Where these disturbances might be the main cause of Sofosbuvir –induced Nephrotoxicity

DISCUSSION

Kidneys are dynamic organs and represent one of the major homeostasis body systems; they are affected by diverse varieties of chemicals and drugs. Sofosbuvir is eliminated by the Kidney and its long time of intake can affect kidney by producing

nephrotoxicity ⁽⁷⁾ . The exact frequency of nephrotoxicity induced by Sofosbuvir is difficult to determine. Direct acting antiviral drugs cause renal failure through a variety of mechanisms. It is related to inhibition of mitochondrial DNA polymerase by intracellular generated triphosphate metabolites of these drugs. Inhibition of renal mitochondrial DNA synthesis leads to impaired mitochondrial ATP synthesis, ATP depletion and impaired oxidative phosphorylation with increased lactic acid production⁽⁸⁾. Sofosbuvir caused renal proximal tubular mitochondrial ultra-structural abnormalities that were parallel to mitochondrial DNA (mtDNA)

depletion in the same cells. Isolation of renal proximal tubules using LCM provided tissue-specific evidence of the compartmentalized toxic effects of Sofosbuvir on renal tubules and localized the toxic site anatomically and molecularly. To our knowledge, this is the first time that mitochondrial toxicity was localized to an anatomically and functionally distinct tissue in a complex organ. Also Crystal deposition in the kidney (mainly increased lactic acid production) may promote the development of renal failure. Other proposed mechanisms of Sofosbuvir nephrotoxicity was the significant decrease in eGFR during treatment in all the studied groups, that was small and reversible after SOF discontinuation ⁽⁹⁾. In an Egyptian hepatitis C cohort study renal cryoglobulinemia occurred with Sofosbuvir treatment. Cryoglobulinemia vasculitis (CryoVas) is a small vessel vasculitis involving the skin, the joints, the peripheral nerve system and the kidneys⁽¹⁰⁾.

In contrast, **Cornella et al.** ⁽¹¹⁾ stated that persistence of mixed cryoglobulinemia despite cure of hepatitis C with new oral antiviral therapy included direct-acting antiviral Sofosbuvir. The most accepted mechanism of Sofosbuvir nephrotoxicity it is incorporated by the mitochondrial RNA polymerase (PolRMT) inhibited mitochondrial protein synthesis and showed a corresponding decrease in mitochondrial oxygen consumption in cells. The nucleoside released by the prodrug Sofosbuvir, was a highly selective inhibitor of mitochondrial RNA transcription. The nucleotide prodrug of Sofosbuvir showed a primary effect on mitochondrial function at sub micro molar concentrations, followed by general cytotoxicity⁽¹²⁾. They

added that the oxidative stress was the major pathway of Sofosbuvir nephrotoxicity. This oxidative stress inhibited the antioxidant enzymes and generated the ROS that destroyed the lipid, protein and DNA components of the cell with subsequent enzymatic inactivation and mitochondrial dysfunction.

Also, accumulation of Sofosbuvir within the cells promotes the generation of the ROS via different pathways. Such ROS might play a role in the pathogenesis of tubular cell apoptosis but probably had no role in the tubular necrosis. Thus, the mechanism of Sofosbuvir -induced renal tubular necrosis was thought to be concentration-dependent ⁽¹³⁾. The current study provided a detailed histological description of the light microscopic and ultra-structural abnormalities in Sofosbuvir Nephrotoxicity.

Sofosbuvir - treated rats revealed 2 types of affection: glomerular (In group III: TDS) and tubular (In group 2: Th.D. S) affections. Where these disturbances might be the main cause of Sofosbuvir

-induced nephrotoxicity Tubular affection (In group 2 Th.D. S) included massive tubular vacuolization especially cells of the proximal and distal convoluted tubule, the lumen of some PCTs contained remnants of degenerated epithelial cells. Their nuclei showed dark staining, with different degrees of degeneration (karyorrhexis, karyolysis or loss). These changes were accompanied with partial affection of glomeruli associated with congestion of glomerular capillaries, widening of the glomerular capsular space. Some of epithelial cells of the proximal and distal tubules showed features of vacuolization. Also there was thickening and edema of vascular wall which filled with blood cells and debris. Some corpuscles showed obliteration of the capsular space or irregular outline of the glomerulus with widening of some areas of the capsular space. Severe damage was observed in other corpuscles in the form of irregularity and shrinkage with loss of their vascular component. **Ray et al.** ⁽¹⁴⁾ reported that Sofosbuvir underwent renal elimination by a combination of glomerular filtration and active tubular secretion. While transporter-mediated uptake of Sofosbuvir from the blood into proximal-tubule cells has been well characterized, comparatively little is known about the efflux system responsible for transporting Sofosbuvir into the lumen during active tubular secretion, so, despite its therapeutic success, renal tubular side effects are reported. **Prasad et al.** ⁽¹³⁾ reported that the light microscopy of Sofosbuvir - treated rats renal sections revealed marked tubular degeneration, necrosis, desquamation of the tubular epithelial cells with cystic formation, interstitial cellular infiltration, wide capsular space and congested glomerular capillary tufts. **Kohler et al.** ⁽¹⁵⁾ concentrated mainly on the proximal convoluted tubules at the cortico-medullary zone and reported the necrotic and apoptotic changes of the renal tubular cells are probably due to the direct effect of the intracellular Sofosbuvir. Moreover, the nephrotoxic effects of Sofosbuvir were more pronounced at the cortico-medullary zone. This might be due to exposure of this zone to a high concentration of Sofosbuvir through the nutrient blood flow to the kidney with subsequent accumulation of a high percentage of the drug within the cells ⁽¹⁵⁾. Glomerular affection (in group III TDS) included marked atrophy, destruction and irregular outline of the glomerulus with widening of some areas of the capsular space, with interstitial edema and hemorrhage. Severe damage was observed in many corpuscles in the form of irregularity and shrinkage with loss of their vascular components. The findings of the present study are in agreement with **Saxena et al.** ⁽¹⁶⁾. In contrast, **Singh et al.** ⁽¹⁷⁾ stated that Sofosbuvir appeared to be generally well tolerated, with minimal nephrotoxicity reported in early studies due to the high safety profile of it. In Recovery Group (R1) who received Th.D. S for three

weeks then left on ordinary diet for another two weeks showed minimal vocalizations in some cells of proximal tubules and the distal tubules. **Brown *et al.*** ⁽¹⁸⁾ found that some of tubules start to return to its normal shape, with preserved brush border of proximal tubule. In Recovery Group (**R2**) who received TDS for three weeks then left on ordinary diet for another two weeks showed healing of some distorted Glomerular tuft of capillaries and some improvement of glomerular and tubular damage. **Bunnell *et al.*** ⁽¹⁹⁾ stated that After Sofosbuvir intake for many months there was minimal vacuolization in some cells of proximal and the distal tubules accompanied with well-preserved brush border of proximal tubule in the rest of the tubules. In the present study, co-administration of (Vitamin C with Sofosbuvir) improved the histopathological findings of Sofosbuvir -induced renal toxicity, where only mild tubular degenerative changes were noticed. The beneficial reno protective effect of vitamin C in Sofosbuvir -treated rats might be due to its antioxidant and / or cyto protective, anti-apoptotic effects ⁽²⁰⁾. **Reeves *et al.*** ⁽²⁰⁾ reported that treatment with IV vitamin C With Sofosbuvir administration protected the kidney against the induced nephrotoxicity, and protective effect of vitamin C was dose dependent.

REFERENCES

- Abdel-Ghaffar TY, Mostafa MS and Suzan El Naghi (2015):** Hepatitis C genotype 4: The past, present, and future. *World Journal of Hepatology*, 7(28): 2792-2799.
- Fabrizi F, Dixit V, Messa P *et al.* (2010):** Pegylated interferon monotherapy of chronic hepatitis C in dialysis patients: Meta- analysis of clinical trials. *Journal of Medical Virology*, 82(5): 768-775.
- Welsch C, Jesudian A, Zeuzem S *et al.* (2012):** New direct-acting antiviral agents for the treatment of hepatitis C virus infection and perspectives. *Gut*, 61(1): 36-46.
- Al Kassaa I, Hober D, Hamze M *et al.* (2014):** Antiviral potential of lactic acid bacteria and their bacteriocins. *Probiotics and Antimicrobial Proteins*, 6(3-4): 177-185.
- Younossi ZM, Stepanova M, Henry L *et al.* (2014):** Effects of sofosbuvir-based treatment, with and without interferon, on outcome and productivity of patients with chronic hepatitis C. *Clinical Gastroenterology and Hepatology*, 12(8): 1349-1359. e1313.
- Padayatty SJ, Katzet A, Wang Y *et al.* (2003):** Vitamin C as an antioxidant: evaluation of its role in disease prevention. *Journal of the American college of Nutrition*, 22(1): 18-35.
- Dashti-Khavidaki S, Khalili H and Nasiri-Toosi M (2018):** Potential nephrotoxicity of sofosbuvir-based treatment in patients infected with hepatitis C virus: a review on incidence, type and risk factors. *Expert Review of Clinical Pharmacology*, 11(5): 525-529.
- Izzedine H, Launay-Vacher V and Deray G (2005):** Antiviral Drug-Induced Nephrotoxicity. *American Journal of Kidney Diseases*, 45(5): 804-817.
- Soeiro CASP, Gonçalves CAM, Marques MSC *et al.* (2018):** Glomerular filtration rate change during chronic hepatitis C treatment with Sofosbuvir/Ledipasvir in HCV/HIV coinfecting patients treated with Tenofovir and a boosted protease inhibitor: an observational prospective study. *BMC Infectious Diseases*, 18(1): 364-372.
- Fayed A, El Nokeety MM, Samy Abdelaziz T *et al.* (2018):** Incidence and characteristics of *de novo* renal cryoglobulinemia after direct-acting antivirals treatment in an Egyptian hepatitis C cohort. *Nephron*, 140:275-281.
- Cornella SL, Stine JG, Kelly V *et al.* (2015):** Persistence of mixed cryoglobulinemia despite cure of hepatitis C with new oral antiviral therapy including direct-acting antiviral sofosbuvir: a case series. *Postgraduate Medicine*, 127(4): 413-417.
- Feng JY, Yili X, Barauskas O *et al.* (2016):** Role of mitochondrial RNA polymerase in the toxicity of nucleotide inhibitors of hepatitis C virus. *Antimicrobial Agents and Chemotherapy*, 60(2): 806-817.
- Prasad N, Patel MR, A. Pandey A *et al.* (2018):** Direct-acting antiviral agents in hepatitis C virus-infected renal allograft recipients: treatment and outcome experience from single center. *Indian Journal of Nephrology*, 28(3): 220-228.
- Ray AS, Cihlar T, Robinson KL *et al.* (2006):** Mechanism of active renal tubular efflux of Sofosbuvir antimicrobial agents and chemotherapy, 50(10): 3297-3304.
- Kohler JJ, Hosseini SH, Hoying-Brandt A *et al.* (2009):** Sofosbuvir renal toxicity targets mitochondria of renal proximal tubules. *Laboratory Investigation*, 89: 513-519.
- Saxena V, Koraisly FM, Sise ME *et al.* (2016):** Safety and efficacy of sofosbuvir- containing regimens in hepatitis C- infected patients with impaired renal function. *Liver International*, 36(6): 807-816.
- Singh T, Soumita B, Kumar Y *et al.* (2016):** Sofosbuvir- based treatment is safe and effective in patients with chronic hepatitis C infection and end stage renal disease: a case series. *Liver International*, 36(6): 802-806.
- Brown PR, Omar S, Alexander W *et al.* (2018):** Acute kidney injury in patients undergoing chronic hepatitis C virus treatment with Ledipasvir/Sofosbuvir. *Hepatology Communications*, 2: 1172-1178.
- Bunnell KL, Vibhakar S, Glowacki RC *et al.* (2016):** Nephrotoxicity associated with concomitant use of ledipasvir- sofosbuvir and tenofovir in a patient with hepatitis C virus and human immunodeficiency virus coinfection. *Pharmacotherapy: The Journal of Human Pharmacology and Drug Therapy*, 36(9): 148-153.
- Yousef JM, Chen G, Hill PA *et al.* (2011):** Ascorbic acid protects against the nephrotoxicity and apoptosis caused by DAAD and affects its pharmacokinetics. *Journal of Antiviral Chemotherapy*, 67(2): 452-459.
- Reeves DJ, Saum LM and Birhiray R (2016):** IV ascorbic acid for treatment of apparent rasburicase-induced methemoglobinemia in a patient with acute kidney injury and assumed glucose-6-phosphate dehydrogenase deficiency. *American Journal of Health-System Pharmacy*, 73(9): 238-242.

